The ATLAS muon and tau triggers

L Dell'Asta[1] on behalf of the ATLAS Collaboration

[1] Boston University, US

E-mail: dellasta@cern.ch

Abstract. The ATLAS experiment at CERN's Large Hadron Collider (LHC) deploys a three-level processing scheme for the trigger system. The development of fast trigger algorithms and the design of topological selections are the main challenges to allow for a large program of physics analyses. In the following, two of the ATLAS trigger signatures are described: the muon and the tau triggers. The structure of the three levels of these two trigger signatures are explained in detail as well as their performance during the first three years of operation.

1. Introduction

ATLAS is one of the two multipurpose experiments at the LHC. Physics goals include the search for the Higgs boson and new physics beyond the Standard Model. The ATLAS detector consists of an inner tracking detector surrounded by a superconducting solenoid which provides a 2 T magnetic field, electromagnetic and hadronic calorimeters and a muon spectrometer with a toroidal magnetic field. More details can be found in Ref. [1].

In 2012, the LHC provided pp collisions at 20 MHz, i.e. every 50 ns. Of the incoming rate, ATLAS recorded approximately 400 Hz for physics analyses. There are various reasons not to record every collision. Firstly, the processes that are of interest to physicists occur at rates of 10, 1 or < 0.1 Hz, which corresponds to a tiny fraction of the total events produced. For example, a process like $H \to ZZ \to \mu\mu\mu\mu$ occurs once in 10^{13} pp interactions (at 14 TeV). Secondly, computing resources are limited. It takes $\sim$10 s to perform the offline processing of one event, so even at just 400 Hz, around 4000 CPUs are needed. Moreover, one event in raw format takes $\sim$1.5 MB, and almost the same size is needed in addition after its reconstruction. With this data size, up to 4300 TB a year per experiment are needed.

The trigger system takes care of selecting, among the 20 MHz of pp collisions, the 400 Hz that will be then analyzed by physicists. The triggers are based on identifying combinations of candidate physics objects (*signatures*), e.g. muons and taus. The trigger system is configured via a trigger *menu* which defines trigger *chains*. A sequence of reconstruction and selection steps for specific objects in the trigger system is specified by a trigger chain which is often referred to as a trigger. Trigger signatures and trigger menus are driven by physics goals. Just to give two examples: the Higgs boson can decay as $H \to ZZ \to \mu\mu\mu\mu$. Therefore a typical signature of the production of the Higgs boson would be the presence of four muons. It is thus important to have a trigger system which can select efficiently events with many muons. Another example is the decay of the Higgs boson in tau pairs, $H \to \tau_{had}\tau_{lep}$. In this case the signature is the presence of an hadronic tau and a lepton, e.g. a muon. A combined trigger is therefore useful.

Interesting events as the ones just described are hidden in the very busy LHC environment. Collisions at the LHC are characterized by high pile-up (i.e. multiple interactions per crossing).

In Table 1 the peak instantaneous luminosities during the first three years of operation are shown. In 2012, when a peak instantaneous luminosity of $7.73 \times 10^{33}\text{cm}^{-2}\text{s}^{-1}$ was reached, events with 35 interactions were recorded, as shown in Fig. 1. When the number of multiple interactions is so high, events are also characterized by a high charged track multiplicity. In Fig. 2 the event display of a $Z \to \mu\mu$ event candidate is shown. The interesting event is overlaid with 25 additional interactions. In such a busy environment several trigger levels are needed to be able to exploit tracking information at the trigger selection.

Table 1. Peak instantaneous luminosities and recorded integrated luminosities during the first three years of ATLAS data taking.

Year	Center of mass energy	Peak Instantaneous Luminosity	Recorded Integrated Luminosity
2010	7 TeV	$2.1 \times 10^{32}\text{cm}^{-2}\text{s}^{-1}$	45.0 pb^{-1}
2011	7 TeV	$3.65 \times 10^{33}\text{cm}^{-2}\text{s}^{-1}$	5.25 fb^{-1}
2012	8 TeV	$7.73 \times 10^{33}\text{cm}^{-2}\text{s}^{-1}$	21.7 fb^{-1}

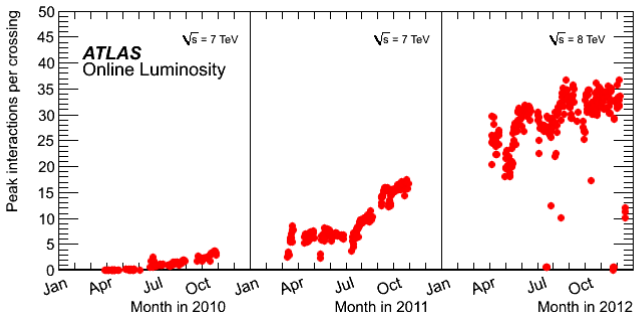

Figure 1. The maximum mean number of events per beam crossing versus day during the *pp* runs of 2010, 2011 and 2012 [2].

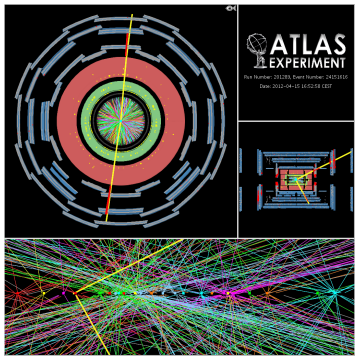

Figure 2. A $Z \to \mu\mu$ candidate event together with 25 additional pile-up reconstructed vertices [3].

The ATLAS trigger system is divided into three levels. At each level, the rate is significantly reduced and more detailed information can be used. The rate reduction factor between the incoming rate and the first level of the trigger is ∼300, while the two following levels have reduction factors of ∼10.

The first level of the trigger system is called Level 1 (L1) and it is hardware-based. It analyzes coarse granularity data from calorimeter and muon detectors separately and identifies Regions-of-Interest (RoI), detector regions to be further analyzed by the High Level Trigger (HLT). After the L1, there is the HLT which is subdivided into two separate levels that are software-based. The Level 2 (L2) accesses the full granularity data within the RoI, which corresponds approximately to 2% of the total event size. At this stage, detector information like tracking is combined. Topological requirements can also be implemented at L2. The Event Filter (EF) uses algorithms similar to offline for object reconstruction. The EF exploits the seed from the L2 and uses the full event data.

In the following, two of the ATLAS trigger signatures are described in detail: the muon and tau triggers.

2. Muon trigger

Muons played a fundamental role in the discovery of the Higgs boson. The discovery announced on the 4th July 2012 (see Ref. [4]) was partly based on the search for the Higgs boson decaying into a Z boson pair, with each Z boson decaying into two muons.

Muons are characterized by the presence of a track in the Muon Spectrometer (MS) and a track in the Inner Detector (ID). ATLAS has specific detectors devoted to triggering these leptons [5].

The Level 1 muon trigger makes use of different detector technologies in different regions of the detector. A quarter-section of the muon system is shown in Fig. 3. The barrel region ($|\eta| < 1.05$) is instrumented with Resistive Plate Chambers (RPC), while the endcap regions ($1.05 < |\eta| < 2.4$) are instrumented with Thin Gap Chambers (TGC). The geometric coverage of the L1 trigger in the endcap regions is ∼99% and ∼80% in the barrel region. The limited geometric coverage in the barrel region is due to a crack at around $\eta = 0$, space used by services of the ID and the calorimeters, the feet and rib support structures of the ATLAS detector and two small elevators at the bottom of the muon spectrometer.

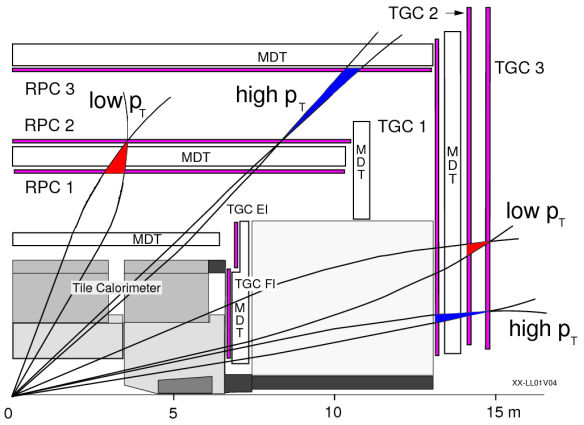

Figure 3. Quarter-section of the muon system in the $z - y$ plane [5].

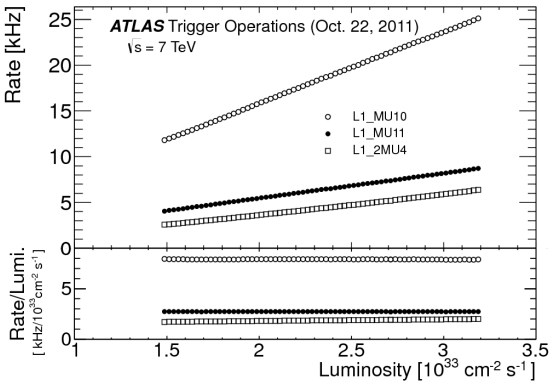

Figure 4. Level 1 muon trigger rates versus the instantaneous luminosity in 2011 [5].

At Level 1, muon candidates are identified by custom-built hardware that forms a coincidence of hits in layers of trigger chambers. The hit pattern along the muon trajectory is used to estimate the transverse momentum, p_{T} , of the muon. Six thresholds were used during 2012: three for high p_{T} (11, 15 and 20 GeV) and three for low p_{T} (4, 6 and 10 GeV). L1 triggers are usually named L1_MUX, where X is the p_{T} threshold in GeV. It is important to note that the low p_{T} thresholds require the coincidence of three layers of muon chambers both in the barrel and in the endcap regions, while the high p_{T} thresholds require two station coincidence in the barrel and three in the endcaps. A L1 muon trigger signal carries the p_{T} information of the muon and the position information of the RoI.

In Fig. 4 the rates for three different L1 triggers as a function of the instantaneous luminosity are shown. It can be seen that L1 rates scale linearly with the instantaneous luminosity, making them robust against pile-up.

Figures 5 and 6 show the L1_MU11 trigger efficiency with respect to offline in the barrel and in the endcap regions respectively. L1_MU11 was one of the main L1 muon triggers used in analyses in 2011. These efficiencies were obtained with a tag-and-probe analysis of $Z \to \mu\mu$

events and they include also the geometric acceptance of the detectors. In the barrel region the efficiencies are lower than in the endcap regions, ∼72.5% and ∼93.5% respectively. The high p_{T} thresholds have 5-10% lower efficiency than the low p_{T} thresholds in the barrel region: this is due to the fact that the latter require the coincidence of only two layers of muon chambers.

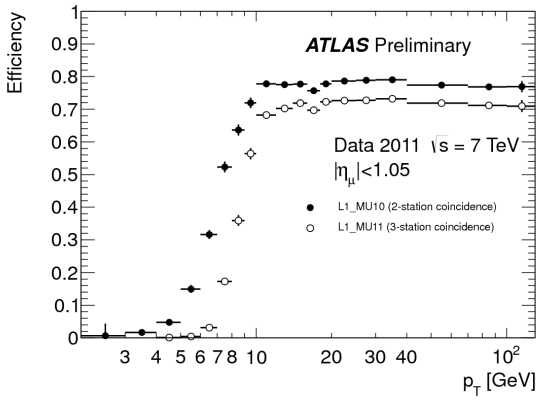

Figure 5. L1 trigger efficiency with respect to isolated offline combined muons for the barrel region as a function of the offline combined muon transverse momentum. The efficiencies include geometric acceptance of the detectors [5].

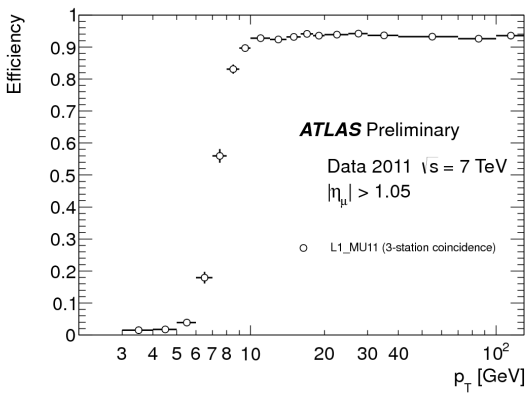

Figure 6. L1 trigger efficiency with respect to isolated offline combined muons for the endcap regions as a function of the offline combined muon transverse momentum. The efficiencies include geometric acceptance of the detectors [5].

At Level 2, the candidate from L1 is refined by using the precision data from the Monitored Drift Tubes (MDT) chambers. The L2 muon standalone algorithm (SA) constructs a track using the MS data within the RoI defined by the L1 seed. First, a pattern recognition algorithm selects hits from the MDT inside the RoI. Second, a track fit is performed using the MDT hits, and a p_{T} measurement is assigned from Look Up Tables (LUTs). Reconstructed tracks in the ID are then combined with the tracks found by the L2 muon SA algorithm by a fast track combination algorithm (CB) to refine the track parameter resolution. Additionally, the isolation algorithm starts from the result of the combined algorithm and incorporates tracking and calorimetric information to find isolated muon candidates (i.e. muons with low near-by activity).

It is essential, for good trigger performance, that the muon track parameters are reconstructed with enough accuracy, i.e. that the track parameters measured online are as close as possible to the ones measured offline, after reconstruction. To evaluate the goodness of the L2 measurements, the resolution of the track parameters is checked. The residuals between the L2 and offline muon track parameters ($1/\ p_{\mathrm{T}}$, η and ϕ) are checked in bins of p_{T} . The widths of the residual distributions are extracted in each bin with a Gaussian fit. The resolution of the inverse p_T track parameter as a function of the offline muon p_T in the barrel is shown in Fig. 7. As expected, the CB algorithm has a better resolution.

Two types of reconstruction algorithms are available at Event Filter. The OutsideIn algorithm starts from the RoI identified by L1 and L2, reconstructing segments and tracks using information from the trigger and precision chambers. The track is then extrapolated back to the beam line to determine the track parameters at the interaction point, thus forming a muon candidate using the MS information only, resulting in the EF standalone trigger. Similar to what is performed by the L2 algorithms, the muon candidate is combined with an ID track to form an EF muon combined trigger. The InsideOut algorithm starts instead from the ID tracks and extrapolates them to the MS region. Due to the extremely busy environment of the ID, the

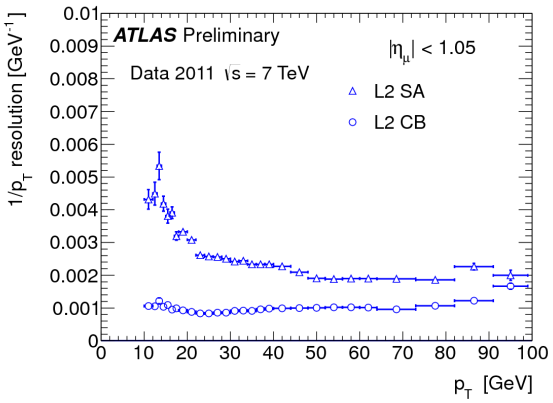

Figure 7. Resolution of the inverse p_T track parameter of the L2 SA and L2 CB algorithms as a function of the offline muon p_T in the barrel region [5].

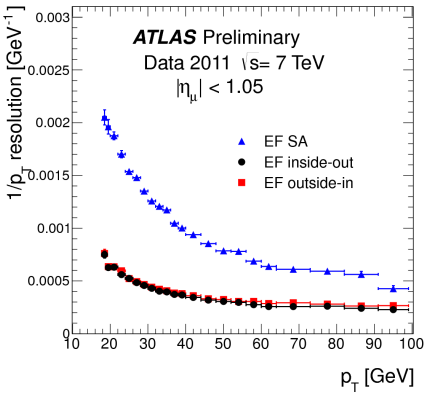

Figure 8. Resolution of the inverse p_T track parameter of the EF SA and EF InsideOut and OutsideIn CB algorithms as a function of the offline muon p_T in the barrel region [5].

InsideOut algorithm is slower, as shown in Fig. 9. The complementary strategies employed by these two algorithms minimize the risk of losing events at the online selection.

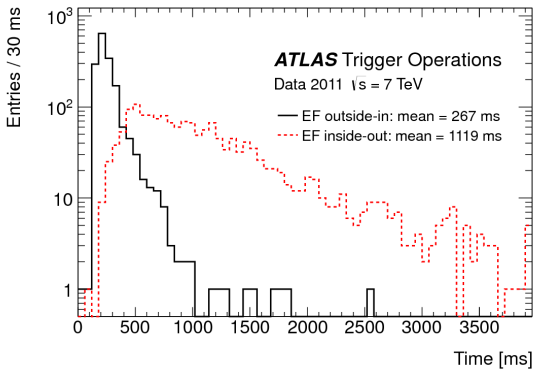

Figure 9. Execution times of the EF OutsideIn (solid line) and InsideOut (dashed line) muon triggers [5].

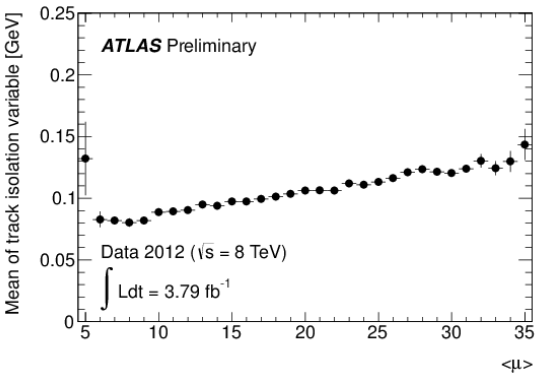

Figure 10. Track isolation variable as a function of number of interactions per bunch crossing [6].

The EF InsideOut and OutsideIn algorithms were running separately during 2011 data taking. To save computing time, in 2012 the two algorithms were merged in a single chain, running the OutsideIn algorithm first and then, if that failed, the InsideOut one.

In addition, isolation algorithms are run at the HLT. These provide a reduction in the rate of the muon trigger while keeping p_T thresholds low. The most critical aspect for isolation algorithms is pile-up robustness. The ATLAS muon trigger has two different types of isolation algorithms. One algorithm is based on information from calorimeters: it uses the energy deposits in the electromagnetic and hadronic calorimeters. The other algorithm uses tracking information: it is based on tracks around the muon candidate. Track based isolation was used in 2012 data taking and it was proved to be pile-up robust (see Fig. 10).

3. Tau trigger

Taus play an important role in the search of the Higgs boson as well as supersymmetric and exotic particles. Taus decay hadronically 65% of the time. Therefore, jets from QCD processes are an overwhelming background to hadronic taus.

Taus can be distinguished from QCD jets: taus are characterized by low track multiplicity and form a narrow, well collimated jet. Tau jets are also isolated: there is no activity around the narrow cone that contains the tau-candidate decay products. These features are exploited by the tau trigger [7].

The Level 1 tau trigger uses electromagnetic (EM) and hadronic (HAD) calorimeter trigger towers with granularity $\Delta\eta \times \Delta\phi = 0.1 \times 0.1$. Hadronic tau decay modes are identified by the following features (shown in Fig. 11): the sum of energy in 2×1 pairs of EM towers, the energy in 2×2 HAD towers behind the EM cluster, the energy in a 4×4 isolation ring around the 2×2 core region. The core region is defined as the two-by-two trigger tower region of $\Delta\eta \times \Delta\phi = 0.2 \times 0.2$. The isolation region is defined as a four-by-four trigger tower region minus a two-by-two core region. In 2012, five different E_{T} thresholds were used: 8, 11, 15, 20, 40 GeV. To keep both the tau trigger rates under control and tau thresholds low, isolation requirements were applied. The absolute E_{T} in the EM isolation region was required to be smaller than 4 GeV.

In Fig. 12 different L1 tau trigger rates as a function of the instantaneous luminosity are shown.

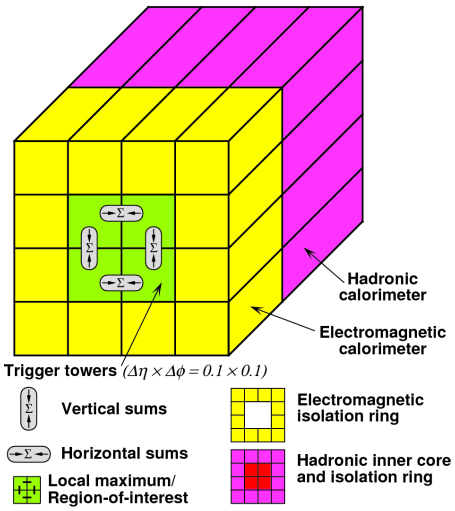

Figure 11. Building blocks of the tau algorithm with the sums to be compared to programmable thresholds.

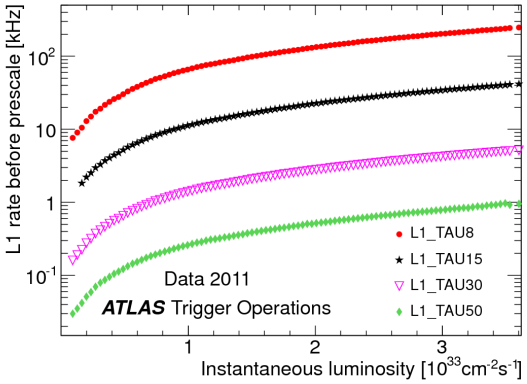

Figure 12. Level 1 tau trigger rates versus the instantaneous luminosity in 2011 [7].

The Level 2 tau trigger uses both calorimetric and tracking information. The calorimeter selection is applied to the RoI. The L2 uses the full granularity information from all layers of the calorimeters within a region of $\Delta\eta \times \Delta\phi = 0.8 \times 0.8$. It refines the position of the RoI and obtains the total E_{T} and shape variables, used to identify hadronically decaying taus. One of these variables is the EM radius, defined as $R_{\mathrm{EM}} = \frac{\sum E\Delta R}{\sum E}$, where the sum extends over all cells in the first three layers of the EM calorimeter. In 2012, in order to improve the algorithm pile-up robustness, the cone used to compute both E_{T} and shape variables changed from 0.4 (used earlier) to 0.2. The effect of this change on the EM radius is shown in Fig. 13. The trigger efficiency as a function of the average number of interactions per bunch crossing is flatter when tightening the cone size.

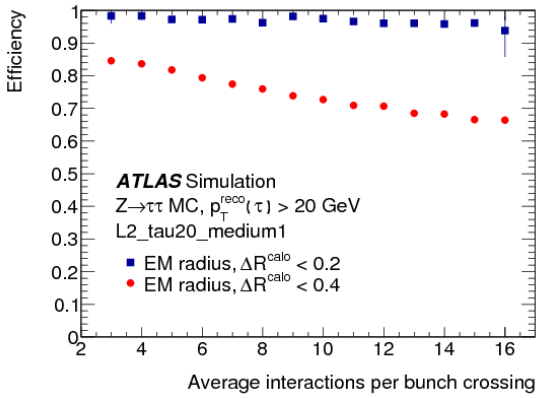

Figure 13. L2 tau trigger efficiencies using the L2 EM radius calculated in cones of $\Delta R < 0.2$ and 0.4 as a function of the average number of interactions per bunch crossing [8].

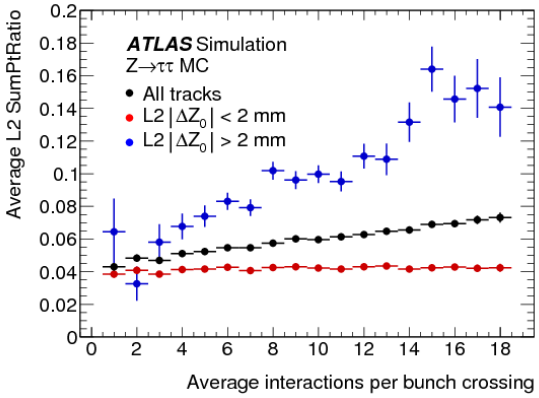

Figure 14. Average L2 SumPtRatio as a function of the average number of interactions per bunch crossing for different track selections [8].

Tracking in the tau RoIs uses fast custom algorithms based on combinatorial pattern recognition followed by a fast Kalman filter track fit. The tracking efficiency is good and comparable to the one found at the Event Filter. Track counting and track-based isolation use tracks found in core and isolation regions of radii 0.1 and 0.3 respectively. One of the tracking variables used to identify taus at L2 is the SumPtRatio, which is the ratio of the scalar sum of the p_{T} of tracks in the isolation region. In 2012, the track selection criteria was changed to improve pile-up robustness: only tracks with an impact parameter compatible ($|\Delta z| < 2$ mm) with the leading track are used. The effect of this improvement is shown in Fig. 14, where the average of the SumPtRatio variable as a function of the average number of interactions per bunch crossing is shown.

At the Event Filter, a more accurate tau reconstruction is performed. In 2011 the hadronic tau identification was cut-based. Cuts were parameterized as a function of E_{T} , number of tracks associated to the tau jet, and track and cluster shape variables. The definition of these variables was the same as the one used by the offline reconstruction. In 2012, to make the online tau identification as similar as possible as in offline, an identification based on multivariate analyses was introduced, using the TMVA Boosted Decision Tree (BDT) (see Ref. [9]). A *medium* identification criteria was chosen, with efficiencies of 85% and 80% for one- and multi-prong taus.

With the new algorithm implementations at L2 and EF, the dependence on pile-up was substantially reduced. Figures 15 and 16 show the efficiency of L1, L2 and EF as a function of the number of reconstructed vertices in 2011 and 2012 data respectively. The efficiency was measured using a tag-and-probe analysis of $Z \to \tau\tau \to \tau_{had} + \mu +$ neutrinos events.

4. Conclusions

In this paper the ATLAS muon and tau triggers have been presented. The ATLAS detector has a three level trigger system, which reduces the incoming rate of 20 MHz LHC collisions to ∼400Hz of recorded data. Trigger signatures and trigger menus are driven by the physics goals, e.g. SM precision measurements and Higgs boson search.

Dedicated muon and tau triggers are available in ATLAS. These triggers were used to select events used in analyses that brought the discovery of a particle compatible with the SM Higgs boson. The description of both triggers and their performance have been shown. The muon

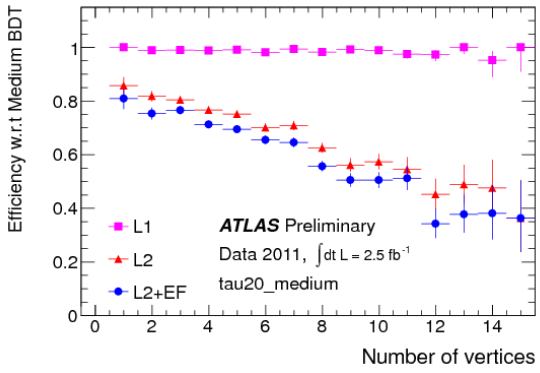

Figure 15. Tau trigger efficiency with respect to offline identified tau candidates as a function of number of vertices measured in 2011 data [8].

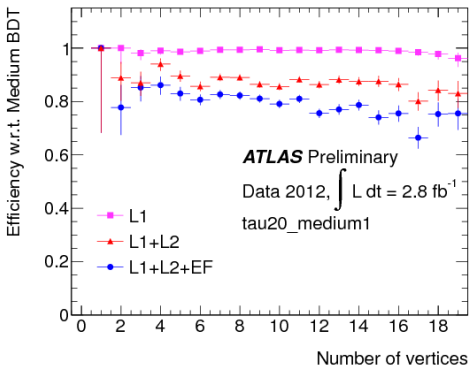

Figure 16. Tau trigger efficiency with respect to offline identified tau candidates as a function of number of vertices measured in 2012 data [8].

trigger combines different detector information and track parameters are measured online with good precision. The trigger efficiency (including the geometric acceptance of the detectors) is approximately 72.5% in the barrel and 93.5% in the endcaps. These efficiensies have been proved to be pile-up robust. The tau trigger is essential for $H \to \tau\tau$ searches. Different algorithms are available in the trigger to help to separate taus from QCD jets. This separation is mainy based both on tracking and calorimeter shape variables. The algorithms used variables that have improved pile-up robustness during the 2012 data taking.

References

[1] The ATLAS Collaboration 2008 The ATLAS Experiment at the CERN Large Hadron Collider *JINST* **3** S08003.

[2] ATLAS Luminosity Public Results web page
`https://twiki.cern.ch/twiki/bin/view/AtlasPublic/LuminosityPublicResults`

[3] ATLAS Event Display web page
`https://twiki.cern.ch/twiki/bin/view/AtlasPublic/EventDisplayStandAlone`

[4] The ATLAS Collaboration 2012 Observation of a new particle in the search for the Standard Model Higgs boson with the ATLAS detector at the LHC *Phys. Lett.* B **716** 1-29

[5] The ATLAS Collaboration 2012 Performance of the ATLAS muon trigger in 2011 ATLAS-CONF-2012-099
`https://atlas.web.cern.ch/Atlas/GROUPS/PHYSICS/CONFNOTES/ATLAS-CONF-2012-099/`

[6] ATLAS Muon Trigger Public Results web page
`https://twiki.cern.ch/twiki/bin/view/AtlasPublic/MuonTriggerPublicResults`

[7] The ATLAS Collaboration 2013 Performance of the ATLAS tau trigger in 2011 ATLAS-CONF-2013-006
`https://atlas.web.cern.ch/Atlas/GROUPS/PHYSICS/CONFNOTES/ATLAS-CONF-2013-006/`

[8] ATLAS Tau Trigger Public Results web page
`https://twiki.cern.ch/twiki/bin/view/AtlasPublic/TauTriggerPublicResults`

[9] Hoecker A, Speckmayer P, Stelzer J, Therhaag J, von Toerne E and Voss H 2007 TMVA: Toolkit for Multivariate Data Analysis *PoS ACAT* **040**